Control of actin dynamics by p38 MAP kinase – Hsp27 distribution in the lamellipodium of smooth muscle cells

Sébastien Pichon, Marijke Bryckaert and Eliane Berrou*

INSERM U 348, IFR Circulation Lariboisière, 41 Boulevard de la Chapelle, 75475 Paris Cedex 10, France

*Author for correspondence (e-mail: eliane.berrou@larib.inserm.fr)

Accepted 19 January 2004
Journal of Cell Science 117, 2569-2577 Published by The Company of Biologists 2004
doi:10.1242/jcs.01110

Summary

We investigated the role of the p38 mitogen-activated protein kinase (p38 MAPK) in the PDGF-BB-induced cytoskeleton remodeling that occurs during the migration of porcine aortic smooth muscle cells (SMC). We showed that p38 MAPK controlled the polymerization of actin that is required for PDGF-induced lamellipodia formation and migration. To investigate the mechanism of action of p38 MAPK, we explored its cellular localization and that of its indirect substrate, the heat shock protein Hsp27, during SMC spreading on fibronectin in the presence and absence of PDGF. Spreading of SMC on fibronectin activated p38 MAPK in a sustained manner only in the presence of PDGF. In these conditions, Hsp27 and p38 MAPK were localized all over the lamellipodia. A transiently phosphorylated form of p38 MAPK was observed at the leading edge, whereas p38 MAPK remained phosphorylated at the base of the lamellipodia. Phosphorylated Hsp27 was excluded from the leading edge and restricted to the base of the lamellipodia. These results were confirmed by Triton X-100 extraction of particulate membrane fraction. Displacement of Hsp27 from the leading edge by cytochalasin D treatment suggests that nonphosphorylated Hsp27 caps barbed ends in vivo. Our data indicate that nonphosphorylated Hsp27 might contribute to the formation of a short, branched actin network at the leading edge, whereas phosphorylated Hsp27 might stabilize the actin network at the base of lamellipodia, which is composed of long, unbranched actin filaments.

Key words: Actin, Cytoskeleton, Migration of smooth muscle cells, p38 MAP kinase, Hsp27

Introduction

The migration of smooth muscle cells (SMC) is a major step in the formation and progression of atherosclerotic lesions. SMC migrate from the media to the intima and accumulate focally as a consequence of the inflammatory response triggered by endothelium injury (Ross, 1999). Among the cytokines and growth factors released from inflammatory cells, platelet-derived growth factor (PDGF) is a potent chemoattractant for SMC (Ross et al., 1990; Schwartz, 1997).

Cell migration involves numerous spatially and temporally coordinated cellular processes and occurs in four steps: the formation of actin-rich protrusions such as lamellipodia, their adhesion, the translocation of the cell body and rear detachment (Lauffenburger and Horwitz, 1996). In vitro reconstitution of actin-based motility requires a minimum set of five pure proteins in addition to actin. These proteins are the Arp2/3 complex, an activator of the Arp2/3 complex that initiates new actin filaments and three actin-binding proteins [actin-depolymerizing factor (ADF)/cofilin, profilin and a capping protein] that enhance the efficiency of treadmilling (Loisel et al., 1999; Pantaloni et al., 2001). In vivo, actin filaments at the leading edge of lamellipodia are organized in a branched network with their barbed ends oriented towards the membrane. Conversely, at the base of lamellipodia actin filaments are long and unbranched (Small et al., 1995; Svitkina and Borisy, 1999). The formation of branched network involves the nucleation of the new filament by an activated Arp2/3 complex, a key event in the production of force and movement. The filament elongates until its barbed end is capped by a capping protein. The binding of Arp2/3 to the pointed ends protects the filaments from depolymerization, which occurs deep within the lamellipodia after the dissociation of Arp2/3 (Pollard and Borisy, 2003). The organization of the actin network therefore requires the spatial regulation of the polymerization/depolymerization of actin filaments, and the distribution of the actin-binding proteins involved in actin dynamics appears to be restricted. In particular, ADF/cofilin depolymerizes F-actin and severs actin filaments (Blanchoin et al., 2000) to create new free barbed ends required for actin nucleation (Chan et al., 2000; Ichetovkin et al., 2002). ADF/cofilin is recruited to the leading edge (Chan et al., 2000). By contrast, tropomyosin inhibits Arp2/3-mediated nucleation (Blanchoin et al., 2001), inhibits the severing activity of cofilin (Ono and Ono, 2002; DesMarais et al., 2002) and allows the annealing of gelsolin-capped filaments, the reverse of severing reaction (Nyakern-Meazza et al., 2002). Tropomyosin is excluded from the leading edge and stabilizes the actin filament at the base of lamellipodia (Des Marais et al., 2002).

However, the mechanisms that regulate lamellipodium

organization are still largely unknown. The small heat shock protein Hsp27 is believed to play a role in the regulation of actin polymerization (Lavoie et al., 1993; Piotrowicz and Levin, 1997), but the molecular basis for its action is not clearly defined. Hsp27 is a substrate of the mitogen-activated protein kinase (MAPK)-activated protein kinases (MK) 2 and 3, which are phosphorylated by p38 MAPK α and β (Guay et al., 1997; Larsen et al., 1997) and required for cell migration (Rousseau et al., 1997; Hedges et al., 1999).

We have previously shown (Berrou and Bryckaert, 2001) that pretreatment of SMC with PDGF inhibits the adhesion of SMC to fibronectin, which is associated with delayed formation of focal complexes and inhibition of stress fiber assembly. The goal of this study was to investigate the mechanism by which p38 MAPK controls PDGF-induced cytoskeleton remodeling. We report that p38 MAPK activity is required for PDGF-induced actin polymerization and chemotaxis of SMC. When SMC spread on fibronectin in the presence of PDGF, p38 MAPK was transiently phosphorylated at the leading edge and remained phosphorylated at the base of the lamellipodia. Phosphorylated Hsp27 was excluded from the leading edge and was restricted to the base of lamellipodia. Furthermore, the localization of nonphosphorylated Hsp27 at the leading edge requires free barbed ends, which is consistent with an actin-capping activity. The distribution of phosphorylated and nonphosphorylated forms of Hsp27 suggests that Hsp27 is involved in the spatial organization of lamellipodia.

Materials and Methods

Reagents and antibodies

Culture media and reagents were obtained from Gibco (Paisley, United Kingdom). Trypsin and soybean trypsin inhibitor were obtained from Worthington Biochemical Corporation (Lakewood, NJ). Fibronectin, Falcon HTS Fluoroblok Inserts (6.4 mm diameter, 8 μm pore size) and mouse monoclonal antibody directed against paxillin were purchased from Becton Dickinson (Bedford, MA). Protein concentrations were determined by the use of a Dc protein assay kit from Biorad (Hercules, CA). Recombinant human PDGF-BB was obtained from R&D Systems (Minneapolis, MN). SB203580 and a polyclonal antibody directed against the phosphorylated form of p38 MAPK were purchased from Promega (Madison, WI). The anti-p38 MAPK polyclonal antibody was obtained from Santa Cruz Biotechnology (Santa Cruz, CA). SB202474, cytochalasin D and latrunculin B were purchased from Calbiochem-Novabiochem (San Diego, CA). The anti-Hsp27 and anti-phospho-Hsp27 (Ser78) polyclonal antibodies were obtained from Stressgen (Victoria, BC, Canada). The anti-p34-Arc polyclonal antibody was obtained from Upstate Biotechnology (Lake Placid, NY). Horseradish peroxidase-conjugated secondary antibodies were purchased from Jackson ImmunoResearch Laboratories (West Grove, PA) and chemiluminescent substrate was purchased from Pierce (Rockford, IL). Alexa Fluor 488-labeled phalloidin, Alexa Fluor 594-labeled DNase I, Alexa Fluor 488-conjugated goat anti-rabbit antibody and the lipophilic carbocyanine dye, CM-Dil, were purchased from Molecular Probes (Eugene, OR). TRITC-phalloidin was purchased from Sigma (St Louis, MI).

Cell culture

Primary cultures of SMC were established from media explants of pig aortas and were subsequently cultured up to seven passages in minimum essential medium with Earle's salts (MEM) supplemented with 2 mM glutamine, 50 units/ml penicillin, 50 μg/ml streptomycin and 10% fetal calf serum. Cultures were rendered quiescent by incubation in serum-free medium containing 0.2% (w/v) BSA for 96 hours. Quiescent SMC were harvested as previously described (Berrou and Bryckaert, 2001) and maintained in suspension in BSA-coated plates for 30 minutes. When appropriate, SB203580 (25 μM) or the related inactive substance SB202474 (25 μM) was added to the suspended cells. PDGF (10 ng/ml) was added when SMC were plated on fibronectin-coated surfaces.

Immunofluorescence microscopy

Suspended SMC were allowed to spread on fibronectin-coated coverslips (25 μg/ml) at 37°C for various times. Adherent cells were fixed in 4% paraformaldehyde for 15 minutes and then permeabilized for 30 minutes in 1% Triton X-100 in permeabilization buffer (300 mM sucrose, 20 mM HEPES, 50 mM NaCl, 3 mM $MgCl_2$, pH 7.0). Cells were then blocked in PBS containing 5% BSA for 1 hour. Filamentous actin was visualized by the use of Alexa 488-labeled phalloidin. A modified protocol was used for cell double labeling. Adherent cells were fixed with 4% paraformaldehyde in cytoskeleton buffer pH 6.9 (0.1 M PIPES, 2 M glycerol, 1 mM EGTA, 1 mM $MgCl_2$) for 15 minutes at room temperature and then permeabilized in the same buffer containing 0.4% Triton X-100 for 20 minutes at room temperature. As the antibody to phosphorylated p38 MAPK (p38 MAPK-P) did not work with paraformaldehyde-fixed cells, SMC were fixed and permeabilized with acetone for 10 minutes at room temperature. This procedure did not affect the cellular distribution of total p38 MAPK. Fixed SMC were then incubated in PBS containing 5% BSA, 2 μM phalloidin and 0.2 μM TRITC-phalloidin for 30 minutes at room temperature. After washings, cells were incubated for 1 hour at 37°C with Hsp27 or phosphorylated Hsp27 (Hsp27-P) polyclonal antibodies or overnight at 4°C with p38 MAPK or p38 MAPK-P polyclonal antibodies. After washings, the cells were incubated with Alexa 488-conjugated goat anti-rabbit antibody for 45 minutes at 37°C.

Determination of F-actin/G-actin ratio

Suspended SMC were transferred to fibronectin-coated wells (5 μg/ml) at a density of 5×10^4 cells/well. After 3 hours at 37°C, SMC were fixed, permeabilized and stained for 30 minutes at room temperature with TRITC-phalloidin at a saturating concentration (2 μM) to stain F-actin or with Alexa Fluor 594-labeled DNase I (3 μM) to stain monomeric G-actin. After three washes with PBS, TRITC-phalloidin and Alexa Fluor 594-labeled DNase I binding were measured on a plate reader (Fluoroscan Ascent FL, Labsystems) at appropriate excitation/emission wavelengths. The background fluorescence estimated before cell labeling was subtracted from the cellular fluorescence measured for each fluorophore. The measurement of F-actin and G-actin contents were linearly related to cell number in the range used for these experiments.

Fluorescence quantification after actin-blocking drug treatments

Cytochalasin D (150 nM) and latrunculin B (80 nM) were added to PDGF-treated SMC for the last 30 minutes of spreading on fibronectin-coated coverslips (25 μg/ml). Then double labeling with TRITC-phalloidin and Hsp27 antibody was performed as described above. Images were analyzed with a macro program (http://www.aecom.yu.edu/aif), using National Institute Health Image software (http://rsb.info.nih.gov/nih-image/). Selected area perimeters were traced by fluorescence threshold in the F-actin channel and also applied to the Hsp27 channel. The macro gives the mean pixel intensity within a 1 pixel (0.18 μm) concentric perimeter running from the outside of the cell to the inside.

Cell migration assay

Cell migration was assessed by use of a modified Boyden chamber with a fluorescence blocking membrane that blocked wavelengths between 490 and 700 nm. Membrane inserts were coated with fibronectin (20 μg/ml) overnight at 4°C. Nonspecific adherence was blocked by incubation with 0.5% BSA in PBS for 1 hour at 37°C. SMC were labeled with a lipophilic carbocyanine, CM-Dil (10 μM), in MEM containing 0.2% BSA 24 hours before carrying out the migration assay. Labeled SMC (5×10^4) suspended in migration medium (MEM without phenol red containing 0.2% BSA) were then transferred to the upper chamber. Migration medium was added to the lower chamber and chemotaxis was induced by adding 10 ng/ml of PDGF to the lower chamber. SB203580 (25 μM), the structurally related inactive substance SB202474 (25 μM) or vehicle were added to both chambers. Fluorescence of migrating cells was measured on a plate reader at excitation/emission wavelengths of 544/590 nm. We checked that fluorescence was linearly related to cell number in the range used for these experiments and that SMC labeling did not affect PDGF activity (results not shown).

Western blot analysis

For the cell spreading on fibronectin experiments, suspended SMC (5×10^5 cells/dish) were plated out on fibronectin-coated culture dishes (5 μg/ml) and incubated at 37°C for different times. Adherent cells were lysed in modified RIPA buffer, pH 7.4 (1% Triton X-100, 1% sodium deoxycholate, 0.1% SDS, 50 mM HEPES, 10% glycerol, 150 mM NaCl, 1.5 mM $MgCl_2$, 1 mM EGTA, 1 mM $NaVO_3$, 100 mM Na_4P2O_7, 100 mM NaF, 10 μg/ml aprotinin and 5 μg/ml leupeptin). The lysates were then clarified by centrifugation at 15,000 ***g*** for 10 minutes at 4°C.

For cell fractionation, quiescent SMC were pre-incubated with SB203580 (25 μM) or vehicle for 30 minutes and stimulated with PDGF (10 ng/ml) for 15 minutes. SMC were extracted by Dounce homogenization in ice-cold hypotonic buffer, pH 7.5 (20 mM HEPES, 10 mM KCl, 1 mM EGTA, 1 mM DTT, 100 μM $NaVO_3$, 50 μM NaF, 10 μg/ml aprotinin and 5 μg/ml leupeptin). Nuclei and unlysed cells were removed by low speed centrifugation (900 ***g***) and the supernatants were then centrifuged at 100,000 ***g*** for 1 hour at 4°C. The pellets were solubilized in 400 μl of cytoskeleton buffer containing 0.04% Triton X-100, 100 μM $NaVO_3$, 50 μM NaF, 10 μg/ml aprotinin and 5 μg/ml leupeptin, and centrifuged again at 100,000 ***g*** for 1 hour at 4°C. The supernatants are referred to as Triton-soluble membrane fractions. The pellets were solubilized in 400 μl of loading buffer and referred to as Triton-insoluble membrane fractions.

The protein concentrations of whole-cell lysates or Triton-soluble membrane fractions were determined. Briefly, 30 μg of whole-cell lysates, 40 μg of Triton-soluble membrane fractions and an equal volume of Triton-insoluble membrane fractions were separated on 12% SDS polyacrylamide gels and immunoblotted according to standard protocols. Bound primary antibodies were visualized by chemiluminescence with appropriate horseradish peroxidase-conjugated secondary antibodies.

Statistics

Data are expressed as the mean±s.e.m. of three independent experiments. Statistical significance was assessed using the Student's *t*-test for paired comparisons.

Results

PDGF-induced actin polymerization requires p38 MAPK activity

To explore further the role of p38 MAPK in the actin cytoskeletal remodeling induced by PDGF, SMC were plated on fibronectin for 3 hours in the presence and absence of PDGF and the F-actin and G-actin contents were determined. The F-actin/G-actin ratio of SMC plated on fibronectin for 3 hours was 47±7% higher in the presence of PDGF than in its absence ($P<0.006$), showing that PDGF stimulated actin polymerization (Fig. 1). In the presence of 25 μM SB203580, a specific inhibitor that fully inhibits p38 MAPK activity (Fig. 3), this increase was abolished ($P>0.09$). By contrast, SB203580 did not modify actin polymerization of control SMC. Similar results were obtained with another inhibitor of p38 MAPK activity, SB202190 (data not shown).

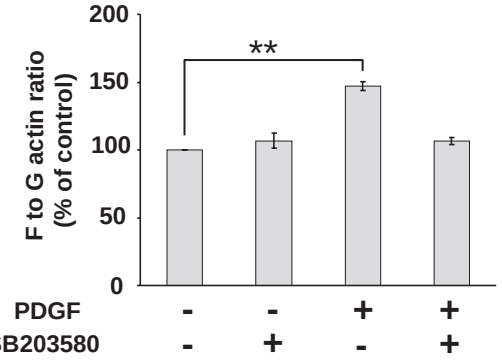

Fig. 1. p38 MAPK is involved in PDGF-induced actin polymerization. Determination of F-actin/G-actin ratio. Suspended SMC were incubated for 30 minutes with 25 μM SB203580 or vehicle and then plated on fibronectin-coated wells for 3 hours in the presence or absence of PDGF (10 ng/ml). Fixed SMC were labeled with TRITC-phalloidin (2 μM) or Alexa 594-DNase I (3 μM). Fluorescence intensities were quantified and relative ratios of F- to G-actin fluorescence were then determined. Data represent the mean±s.e.m. of three independent experiments, carried out in triplicate. **Statistically significant according to Student's *t*-test: $P<0.01$.

These results indicate that p38 MAPK-P is involved in the reorganization of cytoskeleton by controlling the stimulation of actin polymerization induced by PDGF without affecting actin polymerization induced by spreading on fibronectin.

PDGF-induced chemotaxis and lamellipodia formation require p38 MAPK activity

Actin polymerization provides the driving force for the extension of lamellipodia that controls cell movement. Thus, we investigated the role of p38 MAPK in PDGF-induced chemotaxis in SMC.

Cell migration assays were performed with fluorescence-blocking membrane inserts that allowed kinetic studies of cell migration. Chemotaxis towards PDGF (10 ng/ml) was effective for the first 6 hours of the migration assay. After this period, migration of SMC induced by the addition of PDGF to the lower chamber was not significantly different from that induced by the addition of PDGF to both chambers (data not shown). The addition of PDGF to the lower chamber induced a twofold increase ($P<0.005$ compared with the control) in migration of SMC through fibronectin-coated membranes (20 μg/ml) for the 6 hour period during which chemotaxis occurred (Fig. 2A). Pre-incubation of SMC with SB203580 fully inhibited the PDGF-induced migration but did not significantly

affect the basal migration of control SMC, whereas the structurally related inactive substance SB202474 had no effect (data not shown).

To characterize the role of p38 MAPK in the actin cytoskeletal remodeling that allows cell movement, F-actin was visualized by phalloidin staining after 3 hours of spreading of SMC on fibronectin. The addition of PDGF induced the reorganization of the actin cytoskeleton and the formation of motile structures such as lamellipodia (Fig. 2B). Pretreatment of SMC with SB203580 largely abolished the reorganization of cytoskeleton, although small actin protrusions were still observed. SB202474 did not affect PDGF-induced lamellipodia formation.

Thus, the PDGF-induced migration of SMC requires p38 MAK activity, which controls actin polymerization and therefore promotes lamellipodium extension.

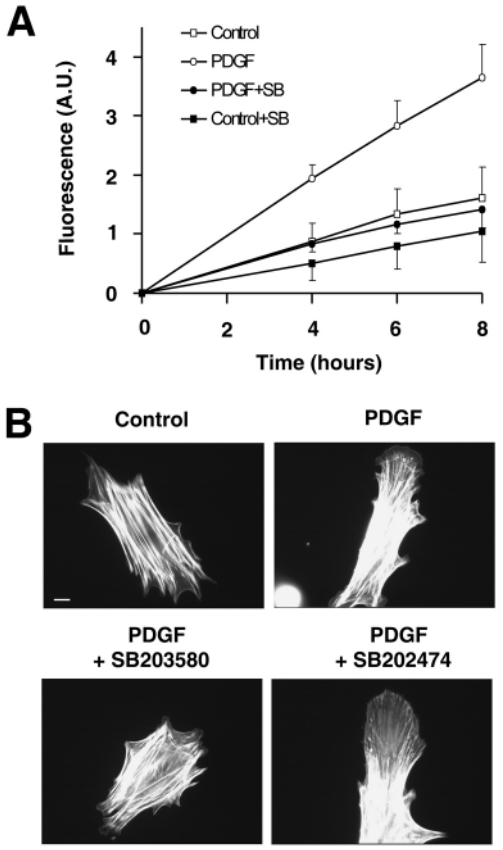

Fig. 2. p38 MAPK is involved in PDGF-induced chemotaxis and cytoskeletal reorganization. (A) Migration assay. Pre-labeled suspended SMC were incubated for 30 minutes with 25 μM SB203580 (SB, closed circles and closed squares), or vehicle (open circles and open squares) and subjected to the migration assay in the presence (circles) or absence (squares) of PDGF (10 ng/ml) in the lower chamber. The fluorescence of migrating cells was determined at different times. Data represent the mean±s.e.m. of three independent experiments, carried out in triplicate. (B) Suspended SMC were incubated for 30 minutes with vehicle, 25 μM SB203580 or 25 μM SB202474 and then plated on fibronectin-coated coverslips for 3 hours in the presence or absence of PDGF (10 ng/ml). SMC were fixed and F-actin was visualized with Alexa 488-phalloidin. Bar, 10 μm. These results are representative of three independent experiments.

Spreading on fibronectin does not induce a sustained activation of p38 MAPK

Although the mechanism by which p38 MAPK controls actin polymerization is unclear, the activation of the p38 MAPK MK2/3 Hsp27 signaling pathway is required (Guay et al., 1997). To explore the role of p38 MAPK in PDGF-induced actin polymerization, we determined the phosphorylation level of Hsp27 and p38 MAPK during cell spreading in the presence and absence of PDGF (Fig. 3). Detachment of SMC resulted in the phosphorylation of Hsp27. Hsp27-P was detected in control SMC 30 minutes after plating on fibronectin. However, the phosphorylation level of Hsp27 dramatically decreased after 3 hours. By contrast, the addition of PDGF induced a sustained phosphorylation of Hsp27, which decreased slightly after 3 hours. Pretreatment of SMC with SB203580 fully inhibited Hsp27 phosphorylation, indicating that Hsp27 phosphorylation is totally dependent on the p38 MAPK pathway whatever the conditions. Interestingly, p38 MAPK phosphorylation increased in the presence of SB203580, possibly because of feedback activation induced by the inhibition of p38 MAPK activity. Determination of the phosphorylation state of p38 MAPK confirmed the requirement of PDGF for sustained activation of p38 MAPK during the spreading of SMC on fibronectin. After 30 minutes, the phosphorylation level of p38 MAPK was similar in control and in PDGF-treated SMC. However, phosphorylation was abolished in control cells after 3 hours, but was still observed in PDGF-treated SMC at this time.

Therefore, the lack of p38 MAPK involvement in actin polymerization induced by SMC spreading on fibronectin was correlated with a lack of sustained p38 MAPK activation. By contrast, the control of actin polymerization by p38 MAPK was correlated with p38 MAPK activity induced by PDGF.

Phosphorylated Hsp27 is excluded from the leading edge

To elucidate the mechanism of action of p38 MAPK, we first investigated the effect of PDGF on the cellular localization

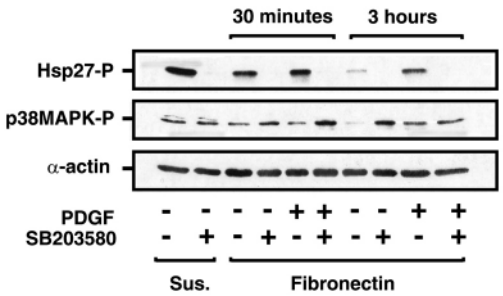

Fig. 3. p38 MAPK activity is not induced by SMC spreading on fibronectin. Suspended SMC were incubated for 30 minutes with 25 μM SB203580 or vehicle and then plated out in dishes coated with fibronectin for 0, 30 minutes and 3 hours in the presence or absence of PDGF (10 ng/ml). SMC lysates (30 μg) were analyzed by immunoblotting using antibodies directed against p38 MAPK-P and Hsp27-P. Blots were reprobed with an anti-α-actin antibody to ensure equal loading. These results are representative of four independent experiments.

of Hsp27 after 3 hours of SMC spreading on fibronectin. When control SMC were labeled with an antibody that recognizes the phosphorylated and the nonphosphorylated forms of Hsp27, it could be seen that Hsp27 was preferentially located in the perinuclear area. Double labeling with Hsp27 antibody and phalloidin indicated that Hsp27 was also detected in lamellipodia induced by PDGF (Fig. 4A). No Hsp27 was found in this location in the presence of SB203580.

To explore further the localization of Hsp27 in the lamellipodia, we compared the distribution of Hsp27 and Hsp27-P. Double labeling with phalloidin and Hsp27 antibody showed overlapping signals, indicating that Hsp27 was present from the base to the edge of lamellipodia. By contrast, it was clear from superimposing Hsp27-P and phalloidin staining in double-labeled SMC that Hsp27-P was excluded from the edge of the lamellipodia (Fig. 4B).

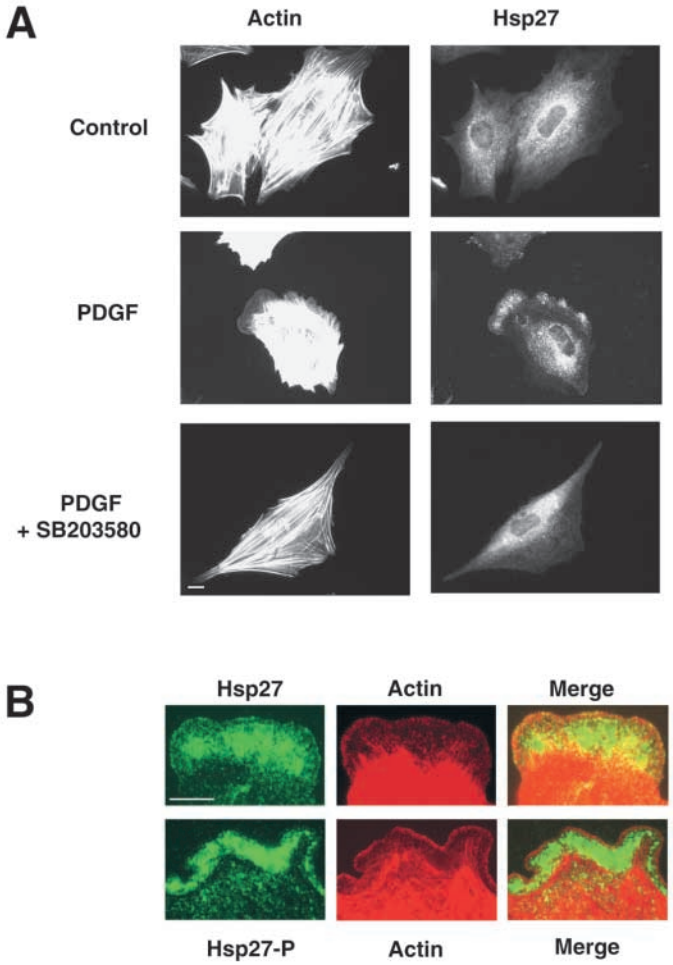

Fig. 4. Hsp27-P is depleted from the leading edge. (A) Suspended SMC were incubated for 30 minutes with 25 μM SB203580 or vehicle and then plated on fibronectin-coated coverslips for 3 hours in the presence or absence of PDGF (10 ng/ml). Fixed SMC were double-labeled for F-actin and Hsp27. Bar, 10 μm. (B) Suspended SMC were plated on fibronectin-coated coverslips for 3 hours in the presence of PDGF. Fixed SMC were double-labeled for F-actin and Hsp27 or Hsp27-P. Bar, 5 μm. These results are representative of three independent experiments.

p38 MAPK is transiently phosphorylated at the leading edge

We next investigated the cellular localization of p38 MAPK. p38 MAPK was observed in the nucleus and cytoplasm of control cells, and also in lamellipodia in PDGF-treated SMC (Fig. 5A). Superimposing p38 MAPK and phalloidin staining indicated that p38 MAPK was present at the leading edge and deeper in the lamellipodia (Fig. 5B). Although p38 MAPK-P staining was always observed at the base of the lamellipodium, two different types of p38 MAPK-P staining were observed at the leading edge. Superimposing p38 MAPK-P and phalloidin staining indicated that p38 MAPK-P was present at the leading edge in some cells but not in others (Fig. 5B).

These results suggest that PDGF-induced p38 MAPK activity triggers the recruitment of p38 MAPK-P to the lamellipodia. However, p38 MAPK was rapidly dephosphorylated at the leading edge and remained phosphorylated at the base of lamellipodia.

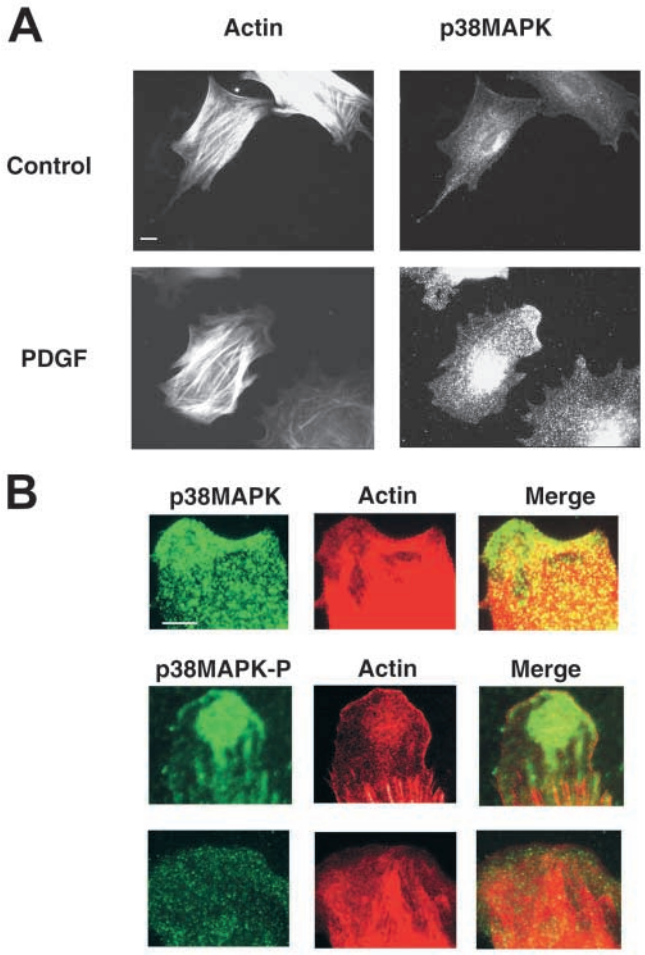

Fig. 5. p38 MAPK is transiently phosphorylated at the leading edge. Suspended SMC were plated on fibronectin-coated coverslips for 3 hours in the presence or absence of PDGF (10 ng/ml). (A) Fixed SMC were double-labeled for F-actin and p38 MAPK. Bar, 10 μm. (B) Fixed SMC were double-labeled for F-actin and p38 MAPK or p38MAPK-P. Bar, 5 μm. These results are representative of three independent experiments.

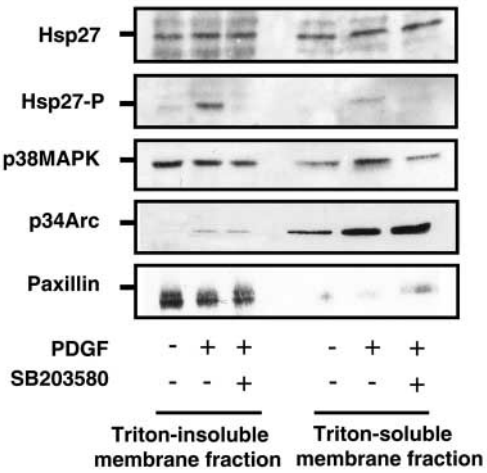

Fig. 6. PDGF induces the recruitment of p38 MAPK in the plasma membrane compartment and the association of Hsp27-P with cortical cytoskeleton. Quiescent SMC were pre-incubated with 25 μM SB203580 or vehicle for 30 minutes and incubated in the presence or absence of PDGF (10 ng/ml) for 15 minutes. Particulate membrane fractions were extracted with 0.04% Triton X-100. Equal volumes of Triton-soluble membrane fraction (40 μg) and Triton-insoluble membrane fraction were analyzed by immunoblotting using antibodies directed against Hsp27, Hsp27-P, p38 MAPK, a component of the Arp 2/3 complex, p34 Arc, and paxillin. These results are representative of two independent experiments.

PDGF induces the recruitment of p38 MAPK in the plasma membrane compartment, which does not contain phosphorylated Hsp27

In parallel, we carried out cell fractionation experiments on quiescent SMC incubated in the presence and absence of PDGF (10 ng/ml) for 15 minutes to determine the cellular distributions of p38 MAPK and Hsp27. Particulate membrane fractions were extracted by 0.04% Triton X-100 to generate a Triton-soluble membrane fraction, which contained plasma membrane-associated proteins, and a Triton-insoluble membrane fraction, which contained cortical cytoskeleton-associated proteins (Fig. 6). Immunoblot analysis indicated that Hsp27 was equally distributed in the Triton-soluble and -insoluble membrane fractions whatever the conditions. By contrast, most Hsp27-P, which was suppressed by SB203580, was detected in the Triton-insoluble membrane fraction of PDGF-treated SMC. The distribution of p38 MAPK was different. The Triton-soluble membrane fraction of PDGF-treated SMC contained more p38 MAPK than did that of untreated cells, and this difference was abolished by SB203580. By contrast, the amount of p38 MAPK in the Triton-insoluble membrane fraction was constant in all conditions tested. Unfortunately, no p38 MAPK-P could be detected in either membrane fraction.

To ensure that Triton X-100 extraction efficiently separated the cortical cytoskeleton compartment from the plasma membrane compartment, we tested two marker proteins: paxillin, which is associated with the cytoskeleton, and p34 Arc, a component of Arp 2/3 complex that promotes actin nucleation and is associated with the plasma membrane. As expected, paxillin was mainly detected in the Triton-insoluble fraction, whereas p34 Arc was found in the Triton-soluble fraction. Moreover, although the paxillin distribution was constant, PDGF induced the recruitment of p34 Arc in the Triton-soluble fraction, which was not inhibited by SB203580.

These results suggested that the Triton-soluble membrane fraction contains proteins involved in actin dynamics and thus localized at the leading edge of lamellipodia, whereas the Triton-insoluble membrane fraction contains proteins associated with the cortical cytoskeleton and thus located deeper in the lamellipodia, a region composed of older actin filaments. Therefore, these results confirm that active p38 MAPK is recruited to the leading edge and that no Hsp27-P is present in the dynamic actin compartment.

Hsp27 localization at the leading edge requires free barbed ends of actin filaments

Hsp27 displays actin-capping activity in vitro, which is inhibited by phosphorylation (Benndorf et al., 1994). Exclusion of Hsp27-P at the leading edge suggested that this mechanism can also occur in vivo. To test this hypothesis, we investigated the requirement of free barbed ends of actin filaments for the localization of Hsp27 at the leading edge. For this, PDGF-treated SMC were exposed to cytochalasin D, which induces actin depolymerization by capping barbed ends (Bear et al., 2002). At the low concentration of cytochalasin D used (150 nM), the stress fibers were partially disrupted and Hsp27 labeling was decreased (Fig. 7A). However, lamellipodia showed minor alterations as assessed by phalloidin, whereas Hsp27 was displaced completely from the leading edge. To ensure that displacement of Hsp27 from the leading edge by cytochalasin D did not result from a general disruption of actin polymerization, we used latrunculin B, which does not interact with free barbed ends but induces actin depolymerization by sequestering actin monomers (Bear et al., 2002). When PDGF-treated SMC were exposed to 80 nM latrunculin B, a decrease in phalloidin staining was observed and bright spots of phalloidin-labeled actin were sometimes detected at the cell periphery or in the cell body (data not shown). However, lamellipodia did not seem to be disrupted. In these conditions, latrunculin B treatment did not affect localization of Hsp27 at the leading edge. Quantification of fluorescence intensities confirmed that depolymerizing agents did not significantly modify F-actin distribution at the leading edge, within 0.90 μm of the membrane (Fig. 7B). Moreover, Hsp27 was associated with actin-containing structures close to the membranes of control and latrunculin B-treated SMC, whereas cytochalasin D treatment displaced Hsp27 from the leading edge. The percentage of fluorescence associated with the plasma membrane decreased from 11.42±0.68% in control cells to 4.29±0.97% in cytochalasin D-treated cells ($P<0.0001$).

Therefore, the localization of nonphosphorylated Hsp27 at the leading edge requires free barbed ends, suggesting strongly that Hsp27 control actin polymerization by acting as a capping protein.

Discussion

We investigated the mechanism by which p38 MAPK controls actin polymerization and lamellipodium formation required for PDGF-induced SMC migration. We found that p38 MAPK is

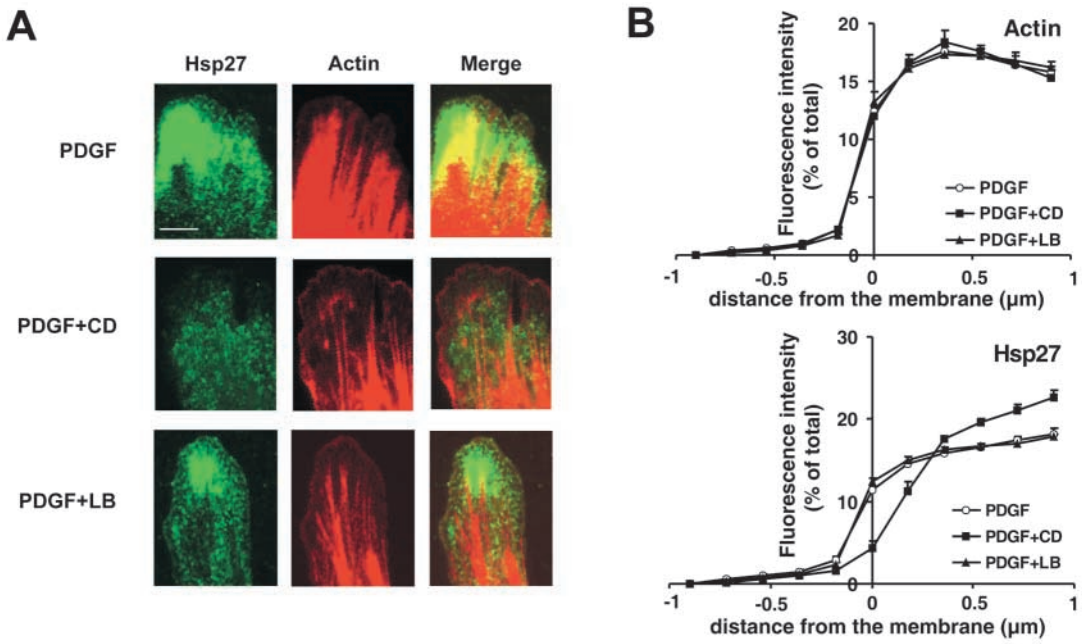

Fig. 7. Hsp27 localization at the leading edge requires free barbed ends. Suspended SMC were plated on fibronectin-coated coverslips for 3 hours in the presence of PDGF (10 ng/ml) and treated with 150 nM cytochalasin D *(*CD, closed squares*)*, 80 nM latrunculin B (LB, closed triangles) or vehicle (open circles), for the last 30 minutes of spreading. (A) Fixed SMC were double-labeled for F-actin and Hsp27. Bar, 5 μm. These results are representative of four independent experiments. (B) Distributions of F-actin and Hsp27 at the leading edge (0.9 μm from the membrane). Results are expressed as a percentage of the total fluorescence for each fluorophore. Data represent the mean±s.e.m. of four independent experiments, carried out on at least ten cells in each experimental condition.

recruited at the leading edge of lamellipodia, the highly dynamic actin compartment. p38 MAPK is transiently phosphorylated, and thus activated, at the leading edge but remains phosphorylated at the base of lamellipodia, whereas Hsp27-P is present only at the base of lamellipodia. On the basis of cytochalasin D displacement experiments, free barbed ends are required for leading edge localization of nonphosphorylated Hsp27. Thus, we propose that Hsp27 displays actin-capping activity in vivo.

Although the p38 MAPK MK2 Hsp27 cascade is known to play a role in cell migration (Rousseau et al., 1997; Hedges et al., 1999), the localization of p38 MAPK in migrating cells had not yet been described. We show for the first time that p38 MAPK is localized at the leading edge and at the base of the lamellipodia in PDGF-treated SMC. Our conclusions are supported by indirect immunofluorescence observations and cell fractionation experiments. Lamellipodia are composed of three zones of actin filament organization: a zone of new branched filaments at the extreme edge, a zone of remodeling and a zone composed of the oldest and longest filaments (Pollard and Borisy, 2003). Triton X-100 solubilizes membrane-associated proteins and short, branched filaments, but not cross-linked filaments (Small et al., 1995; Watts, 1995). Therefore, the Triton-soluble membrane fraction included proteins that control actin polymerization that are associated with actin filaments at the leading edge of lamellipodia (e.g. the Arp2/3 complex). By contrast, the Triton-insoluble membrane fraction contained proteins such as paxillin, a component of focal complexes, which is associated with actin filaments located deeper within lamellipodia. We showed that recruitment of p38 MAPK to the plasma membrane requires its activity. In accordance with this result, it was recently reported that as well as requiring catalytic activity, cell migration requires the N-terminal proline-rich domain of the substrate of p38 MAPK, MK2, which might target the serine/threonine kinase to the actin polymerization site (Kotlyarov et al., 2002). Inactive p38 MAPK is associated with MK2 in the nucleus (Ben-Levy et al., 1998). Phosphorylation of MK2 unmasks a nuclear export signal, resulting in transport of the p38 MAPK-MK2 complex from the nucleus to the cytoplasm (Engel et al., 1998). However, recent reports suggest that p38 MAPK is activated outside the nucleus (Rane et al., 2001; Buchsbaum et al., 2002). The amount of p38 MAPK in the Triton-insoluble membrane fraction was constant whatever the conditions. Although we cannot rule out the possibility that p38 MAPK had residual activity, our results suggest that p38 MAPK is associated with the cytoskeleton independently of its activity. Whatever the p38 MAPK activating pathway, immunofluorescence observations suggest that p38 MAPK is rapidly dephosphorylated after being recruited at the leading edge but remains active at the base of lamellipodia.

Monomeric Hsp27 displays actin-capping activity in vitro, which is inhibited by multimeric organization and the phosphorylation of Hsp27 (Miron et al., 1988; Benndorf et al., 1994). In vivo, growth factor-induced actin polymerization and cytoskeleton remodeling do not take place in cells expressing nonphosphorylatable Hsp27 (Lavoie et al., 1993; Piotrowicz and Levin, 1997; Piotrowicz et al., 1998). Our results indicate that Hsp27 is distributed all over the lamellipodia, whereas Hsp27-P is excluded from the leading edge, where actin polymerization is controlled. Moreover, we showed that low doses of cytochalasin D, which preferentially cap barbed ends

(Sampath and Pollard, 1991), displaced nonphosphorylated Hsp27 from the leading edge, providing the first evidence of actin-capping activity of Hsp27 in vivo. Thus, the signaling pathway that promotes actin-capping activity must include the following steps: phosphorylation of Hsp27 by MK2, leading to the dissociation of large oligomers that are present in vivo (Lambert et al., 1999), and rapid dephosphorylation, which allows Hsp27 to interact with actin barbed ends. Two lines of evidence are consistent with this mechanism. First, capping proteins are required for actin polymerization and efficient motility (Loisel et al., 1999). By limiting the length of the growing branches, capping proteins contribute to generate efficient propulsive forces (Pollard and Borisy, 2003). Moreover, capping proteins cap most of the barbed ends. Disassembly of many capped filaments increases the concentration of monomeric ATP-actin and thus allows the growth of a few barbed ends (Pantaloni et al., 2001). Second, motility is higher in cells that overexpress Hsp27 (Piotrowicz et al., 1998) or capping proteins from the gelsolin family (Cunningham et al., 1991; Sun et al., 1995; Furnish et al., 2001).

Our results indicate that the p38 MAPK cascade is involved in PDGF-induced actin polymerization, but not in the polymerization that occurs during SMC spreading, suggesting that a different pathway is involved. In accordance with our results, fibroblasts from the gelsolin-null mice contain many stress fibers but are defective in actin polymerization and lamellipodia formation after growth factor stimulation (Azuma et al., 1998).

Therefore, Hsp27 might play a specific role in the regulation of actin polymerization mediated by the Arp2/3 complex. Moreover, Hsp27 might be involved in the spatial organization of lamellipodia. The amount of branched actin filaments appears to increase with increasing concentrations of gelsolin in vitro (Wiesner et al., 2003). Thus, at the dynamic leading edge, Hsp27 might promote branching array by its actin-capping activity. Furthermore, the phosphorylation of Hsp27 is essential for stabilization of the actin cytoskeleton during heat shock (Lavoie et al., 1995). At the base of lamellipodia, p38 MAPK remains active and Hsp27 is phosphorylated and might stabilize actin filaments by directly or indirectly interacting with F-actin (Mounier and Arrigo, 2002). Indirect interactions might involve tropomyosin, which appears to be restricted to the base of lamellipodia (DesMarais et al., 2002). Tropomyosin stabilizes actin filaments and protects them from ADF/cofilin severing and Arp2/3 complex-nucleated branching, which only occur at the leading edge. Interestingly, during SMC contraction, the phosphorylation of Hsp27 increases the binding of Hsp27 to tropomyosin (Bitar, 2002).

In conclusion, our study indicates that the p38 MAPK cascade controls actin polymerization required for PDGF-induced SMC migration. Exclusion of phosphorylated Hsp27 from the leading edge correlating with the requirement of free barbed ends of actin filaments for localization of nonphosphorylated Hsp27 at the leading edge suggest strongly that Hsp27 controls actin polymerization by acting as a capping protein. Hsp27 might contribute to the spatial organization of lamellipodia by promoting branch formation at the leading edge and filament stability at the base.

This work was supported by the Association pour la Recherche contre le Cancer (ARC, contract number 5820) and the Fondation Simone et Cino del Duca. S.P. is supported by fellowships from the Groupe d'Etudes sur l'Hémostase et la Thrombose (GEHT) and the Nouvelle Société Française de l'Athérosclérose (NSFA).

References

Azuma, T., Witke, W., Stossel, T. P., Hartwig, J. H. and Kwiatkowski, D. J. (1998). Gelsolin is a downstream effector of rac for fibroblast motility. *EMBO J.* **17**, 1362-1370.

Bear, J. E., Svitkina, T. M., Krause, M., Schafer, D. A., Loureiro, J. J., Strasser, G. A., Maly, I. V., Chaga, O. Y., Cooper, J. A., Borisy, G. G. et al. (2002). Antagonism between Ena/VASP proteins and actin filament capping regulates fibroblast motility. *Cell* **109**, 509-521.

Ben-Levy, R., Hooper, S., Wilson, R., Paterson, H. and Marshall, C. (1998). Nuclear export of the stress-activated protein kinase p38 mediated by its substrate MAPKAP kinase-2. *Curr. Biol.* **8**, 1049-1057.

Benndorf, R., Hayess, K., Ryazantsev, S., Wieske, M., Behlke, J. and Lutsch, G. (1994). Phosphorylation and supramolecular organization of murine small heat shock protein HSP25 abolish its actin polymerization-inhibiting activity. *J. Biol. Chem.* **269**, 20780-20784.

Berrou, E. and Bryckaert, M. (2001). Platelet-derived growth factor inhibits smooth muscle cell adhesion to fibronectin by ERK-dependent and ERK-independent pathways. *J. Biol. Chem.* **276**, 39303-39309.

Bitar, K. N. (2002). HSP27 phosphorylation and interaction with actin-myosin in smooth muscle contraction. *Am. J. Physiol. Gastrointest. Liver Physiol.* **282**, G894-G903.

Blanchoin, L., Pollard, T. and Mullins, R. (2000). Interactions of ADF/cofilin, Arp2/3 complex, capping protein and profilin in remodeling of branched actin filament networks. *Curr. Biol.* **10**, 1273-1282.

Blanchoin, L., Pollard, T. D. and Hitchcock-DeGregori, S. E. (2001). Inhibition of the Arp2/3 complex-nucleated actin polymerization and branch formation by tropomyosin. *Curr. Biol.* **11**, 1300-1304.

Buchsbaum, R. J., Connolly, B. A. and Feig, L. A. (2002). Interaction of Rac exchange factors Tiam1 and Ras-GRF1 with a scaffold for the p38 mitogen-activated protein kinase cascade. *Mol. Cell. Biol.* **22**, 4073-4085.

Chan, A. Y., Bailly, M., Zebda, N., Segall, J. E. and Condeelis, J. S. (2000). Role of cofilin in epidermal growth factor-stimulated actin polymerization and lamellipod protrusion. *J. Cell Biol.* **148**, 531-542.

Cunningham, C., Stossel, T. and Kwiatkowski, D. (1991). Enhanced motility in NIH 3T3 fibroblasts that overexpress gelsolin. *Science* **251**, 1233-1236.

DesMarais, V., Ichetovkin, I., Condeelis, J. and Hitchcock-DeGregori, S. E. (2002). Spatial regulation of actin dynamics: a tropomyosin-free, actin-rich compartment at the leading edge. *J. Cell Sci.* **115**, 4649-4660.

Engel, K., Kotlyarov, A. and Gaestel, M. (1998). Leptomycin B-sensitive nuclear export of MAPKAP kinase 2 is regulated by phosphorylation. *EMBO J.* **17**, 3363-3371.

Furnish, E., Zhou, W., Cunningham, C., Kas, J. and Schmidt, C. (2001). Gelsolin overexpression enhances neurite outgrowth in PC12 cells. *FEBS Lett.* **508**, 282-286.

Guay, J., Lambert, H., Gingras-Breton, G., Lavoie, J., Huot, J. and Landry, J. (1997). Regulation of actin filament dynamics by p38 map kinase-mediated phosphorylation of heat shock protein 27. *J. Cell Sci.* **110**, 357-368.

Hedges, J. C., Dechert, M. A., Yamboliev, I. A., Martin, J. L., Hickey, E., Weber, L. A. and Gerthoffer, W. T. (1999). A role for p38MAPK/HSP27 pathway in smooth muscle cell migration. *J. Biol. Chem.* **274**, 24211-24219.

Ichetovkin, I., Grant, W. and Condeelis, J. (2002). Cofilin produces newly polymerized actin filaments that are preferred for dendritic nucleation by the Arp2/3 complex. *Curr. Biol.* **12**, 79-84.

Kotlyarov, A., Yannoni, Y., Fritz, S., Laass, K., Telliez, J.-B., Pitman, D., Lin, L.-L. and Gaestel, M. (2002). Distinct cellular functions of MK2. *Mol. Cell. Biol.* **22**, 4827-4835.

Lambert, H., Charette, S. J., Bernier, A. F., Guimond, A. and Landry, J. (1999). HSP27 Multimerization mediated by phosphorylation-sensitive intermolecular interactions at the amino terminus. *J. Biol. Chem.* **274**, 9378-9385.

Larsen, J. K., Yamboliev, I. A., Weber, L. A. and Gerthoffer, W. T. (1997). Phosphorylation of the 27-kDa heat shock protein via p38 MAP kinase and MAPKAP kinase in smooth muscle. *Am. J. Physiol. Lung Cell Mol. Physiol.* **273**, L930-L940.

Lauffenburger, D. and Horwitz, A. (1996). Cell migration: a physically integrated molecular process. *Cell* **84**, 359-369.

Lavoie, J., Hickey, E., Weber, L. and Landry, J. (1993). Modulation of actin

microfilament dynamics and fluid phase pinocytosis by phosphorylation of heat shock protein 27. *J. Biol. Chem.* **268**, 24210-24214.

Lavoie, J., Lambert, H., Hickey, E., Weber, L. and Landry, J. (1995). Modulation of cellular thermoresistance and actin filament stability accompanies phosphorylation-induced changes in the oligomeric structure of heat shock protein 27. *Mol. Cell. Biol.* **15**, 505-516.

Loisel, T., Boujemaa, R., Pantaloni, D. and Carlier, M. (1999). Reconstitution of actin-based motility of *Listeria* and *Shigella* using pure proteins. *Nature* **401**, 613-616.

Miron, T., Wilchek, M. and Geiger, B. (1988). Characterization of an inhibitor of actin polymerization in vinculin-rich fraction of turkey gizzard smooth muscle. *Eur. J. Biochem.* **178**, 543-553.

Mounier, N. and Arrigo, A. (2002). Actin cytoskeleton and small heat shock proteins: how do they interact? *Cell Stress Chaperones* **7**, 167-176.

Nyakern-Meazza, M., Narayan, K., Schutt, C. E. and Lindberg, U. (2002). Tropomyosin and gelsolin cooperate in controlling the microfilament system. *J. Biol. Chem.* **277**, 28774-28779.

Ono, S. and Ono, K. (2002). Tropomyosin inhibits ADF/cofilin-dependent actin filament dynamics. *J. Cell Biol.* **156**, 1065-1076.

Pantaloni, D., Le Clainche, C. and Carlier, M. (2001). Mechanism of actin-based motility. *Science* **292**, 1502-1506.

Piotrowicz, R. S. and Levin, E. G. (1997). Basolateral membrane-associated 27-kDa heat shock protein and microfilament polymerization. *J. Biol. Chem.* **272**, 25920-25927.

Piotrowicz, R. S., Hickey, E. and Levin, E. G. (1998). Heat shock protein 27 kDa expression and phosphorylation regulates endothelial cell migration. *FASEB J.* **12**, 1481-1490.

Pollard, T. and Borisy, G. (2003). Cellular motility driven by assembly and disassembly of actin filaments. *Cell* **112**, 453-465.

Rane, M. J., Coxon, P. Y., Powell, D. W., Webster, R., Klein, J. B., Pierce, W., Ping, P. and McLeish, K. R. (2001). p38 kinase-dependent MAPKAPK-2 activation functions as 3-phosphoinositide-dependent kinase-2 for Akt in human neutrophils. *J. Biol. Chem.* **276**, 3517-3523.

Ross, R. (1999). Atherosclerosis – an inflammatory disease. *N. Engl. J. Med.* **340**, 115-126.

Ross, R., Masuda, J., Raines, E., Gown, A., Katsuda, S., Sasahara, M., Malden, L., Masuko, H. and Sato, H. (1990). Localization of PDGF-B protein in macrophages in all phases of atherogenesis. *Science* **248**, 1009-1012.

Rousseau, S., Houle, F., Landry, J. and Huot, J. (1997). p38 MAP kinase activation by vascular endothelial growth factor mediates actin reorganization and cell migration in human endothelial cells. *Oncogene* **15**, 2169-2177.

Sampath, P. and Pollard, T. (1991). Effects of cytochalasin, phalloidin, and pH on the elongation of actin filaments. *Biochemistry* **30**, 1973-1980.

Schwartz, S. (1997). Smooth muscle migration in atherosclerosis and restenosis. *J. Clin. Invest.* **100**, S87-S89.

Small, J., Herzog, M. and Anderson, K. (1995). Actin filament organization in the fish keratocyte lamellipodium. *J. Cell Sci.* **129**, 1275-1286.

Sun, H., Kwiatkowska, K., Wooten, D. and Yin, H. (1995). Effects of CapG overexpression on agonist-induced motility and second messenger generation. *J. Cell Biol.* **129**, 147-156.

Svitkina, T. M. and Borisy, G. G. (1999). Arp2/3 complex and actin depolymerizing factor/cofilin in dendritic organization and treadmilling of actin filament array in lamellipodia. *J. Cell Biol.* **145**, 1009-1026.

Watts, R. (1995). Role of gelsolin in the formation and organization of triton-soluble F-actin during myeloid differentiation of HL-60 cells. *Blood* **85**, 2212-2221.

Wiesner, S., Helfer, E., Didry, D., Ducouret, G., Lafuma, F., Carlier, M.-F. and Pantaloni, D. (2003). A biomimetic motility assay provides insight into the mechanism of actin-based motility. *J. Cell Biol.* **160**, 387-398.